Serum and Urinary Metabonomic Study of Human Osteosarcoma

ARTICLE *in* JOURNAL OF PROTEOME RESEARCH · SEPTEMBER 2010

Impact Factor: 4.25 · DOI: 10.1021/pr100480r · Source: PubMed

15 AUTHORS, INCLUDING:

Yunping Qiu
Yeshiva University
79 PUBLICATIONS **3,011** CITATIONS
SEE PROFILE

Li Pan
Purdue University
8 PUBLICATIONS **62** CITATIONS
SEE PROFILE

Wei Jia
University of Hawai'i at Mānoa
263 PUBLICATIONS **6,126** CITATIONS
SEE PROFILE

technical notes Journal of proteome research

Serum and Urinary Metabonomic Study of Human Osteosarcoma

Zhiyu Zhang,[§,†,#] Yunping Qiu,[‡,#] Yingqi Hua,[§,||,#] Yihuang Wang,[▽,#] Tianlu Chen,[⊥] Aihua Zhao,[⊥] Yi Chi,[⊥] Li Pan,[⊥] Shuo Hu,[||] Jian Li,[||] Chengwei Yang,[||] Guodong Li,[§] Wei Sun,[§] Zhengdong Cai,[*,§,||] and Wei Jia[*,‡]

Shanghai 10th People's Hospital, Tongji University School of Medicine, Shanghai 200072, P. R. China, Department of Orthopedics, The 4th Affiliated Hospital, China Medical University, Shenyang, 110032, P. R. China, Department of Nutrition, University of North Carolina at Greensboro, North Carolina Research Campus, Kannapolis NC 28081, Department of Orthopedics, The Changhai Hospital of Second Military Medical University, Shanghai 200433, P. R. China, School of Pharmacy, and Ministry of Education Key Laboratory of Systems Biomedicine, Shanghai Center for Systems Biomedicine, Shanghai Jiao Tong University, Shanghai, 200240, P. R. China, and State Key Laboratory for Medical Genomics, Institute of Health Sciences, Shanghai Institutes for Biological Sciences, Graduate School of the Chinese Academy of Sciences, and Shanghai Institute of Hematology, RuiJin Hospital, Shanghai Jiao Tong University School of Medicine, Shanghai, 200240, P. R. China

Received May 16, 2010

Abstract: Osteosarcoma (OS) is the most common malignant bone tumor found in children. Currently, researchers have focused on protein and gene levels, while the associated metabolic variations have been poorly understood. In this study, we used a gas chromatography mass spectrometry approach and profiled small-molecule metabolites in serum and urine of 24 OS patients, 19 benign bone tumor patients, and 32 healthy controls, to determine whether there are significant alterations associated with carcinogenesis. The metabonomic results demonstrate clear intergroup separations between healthy control subjects and bone tumor patients in the orthogonal partial least-squares-discriminant analysis (OPLS-DA) models. Differential metabolites identified from the metabonomic analysis suggest a disrupted energy metabolism in OS patients, as characterized by significantly down-regulated TCA cycle and glycolysis, down-regulated lipid metabolism, dysregulated sugar levels, and up-regulated amino acid metabolism. Additionally, an increased activity of glutathione metabolism, and increased polyamine metabolism also contributed to a characteristic metabolic signature of OS patients.

Keywords: osteosarcoma • gas chromatography−mass spectrometry•serum•urine•metabolomics•metabonomics

Introduction

Osteosarcoma (OS) is a primary malignant bone tumor that usually develops in children and young adults during periods of rapid growth. It most frequently occurs in the second decade of life; about 60% of patients are under 25 years old, whereas only 30% are over 40.[1] OS represents about 0.2% all malignant tumors with an incidence of 3 cases/million population/year.[2] OS tumors are located in the metaphyseal regions of long bones, where the distal femur, proximal tibia, and proximal humerus are the three most common sites.[3] Although the introduction of neoadjuvant chemotherapy has greatly improved the treatment of this tumor, the long-term survival rate remains about 60−70%.[4] Early detection and treatment, as well as a better understanding of its global biochemical dysregulations are of great importance in enhancing the clinical efficacy of OS therapy.

Much research has been done on gene and protein levels to understand the pathogenesis and development of OS, which has identified many OS related genes and proteins related to familial genetics, cell cycle biology, DNA damage pathways, and the use of chemotherapy.[5−8] However, alterations at the level of small-molecule metabolites, the downstream end points of these genes and proteins, have been poorly delineated. The advent of metabonomics technology utilizing advanced analytical instruments and statistical tools enables researchers to acquire high-throughput metabolite data sets and demonstrate them as simple mathematical models with global biochemical information. Despite its relatively short history, metabonomics has been successfully utilized in the understanding and biomarker detection of many diseases, including colorectal cancer,[9,10] prostate cancer,[11] lung cancer,[12] kidney cancer,[13] inflammatory bowel disease,[14] type 2 diabetes,[15] and so on. Therefore, we sought to determine if significant variations in metabolites in the biofluids associated with OS morbidity can be identified in OS patients, and comprehensively characterized by a metabonomic approach.

To test this hypothesis, we used gas chromatography−mass spectrometry (GC-MS) based metabonomic platforms to profile metabolites in serum and urine samples from OS patients,

* To whom correspondence should be addressed. Zhengdong Cai, Musculoskeletal Oncology Center, Shanghai 10th People's Hospital, Tongji University School of Medicine, Shanghai 200072, China. Phone: 86-21-66307330. Fax: 86-21-66307330. E-mail: zhdcai@gmail.com. Wei Jia, Department of Nutrition, University of North Carolina at Greensboro, North Carolina Research Campus, Kannapolis NC 28081, USA. Phone: 1-704-250-5803. Fax: 1-704-250-5809. E-mail: w_jia@uncg.edu.

§ Tongji University School of Medicine.

† China Medical University.

# These authors contributed equally to this work.

‡ University of North Carolina at Greensboro.

|| The Changhai Hospital of Second Military Medical University.

▽ Shanghai Jiao Tong University School of Medicine.

⊥ Shanghai Jiao Tong University.

10.1021/pr100480r

Published on Web 07/20/2010

Table 1. Tumor Type and Age Range Information for Patients

tumor type	age (14−30)	age (30−50)	age (>50)
Osteosarcoma	21	3(35, 44,47)	
Giant cell tumor	10	2(39,43)	
Chondrosteoma	1(29)		1(76)
Aneurysmal bone cyst		1(42)	
Chondromyxoidfibroma	1(29)		
Enchondroma			1(61)
Osteofibrous dysplasia			1(75)
Unicameral bone cyst			1(72)

benign bone tumor patients, and healthy controls. The study intended to discover the important metabolite markers associated with OS morbidity, which could be utilized for improved OS detection, prognosis, and therapeutic strategies.

Materials and Methods

Chemicals. Methoxyamine HCl, Bis(Trimethylsilyl)-Trifluoroacetamide (BSTFA, with 1% Trimethylchlorosilane, TMCS), and heptadecanoic acid were purchased from Sigma-Aldrich. Ethyl chloroformate (ECF), pyridine, anhydrous ethanol, sodium hydroxide, chloroform, and anhydrous sodium sulfate were analytical grade from China National Pharmaceutical Group Corporation (Shanghai, China). L-2-chlorophenylalanine was purchased from Intechem Tech. Co. Ltd. (Shanghai, China).

Patients and Samples. Serum and urine samples were collected from 24 OS patients (13 males and 11 females), whose mean age was 19.2 years old (age range 14−47, most in the 14−20 range), 19 benign bone tumor patients (10 males and 9 females), whose mean age was 37 years (age range 16−76, most in the 16−30 range). They were compared to a control group of 32 healthy individuals (17 males and 15 females), with a mean age of 18.6 years (age range 15−21). Specific information about tumor types and ages are shown in Table 1. Diagnosis for all patients was confirmed by pathological examinations. Sample collection was conducted following a Tong University IRB-approved protocol after all participants signed written informed consent. All patients were not on any medical treatment for 2 weeks prior to sample collection. All samples were collected in the morning before breakfast. Urine samples were immediately frozen with dry ice, and sera were separated from vein blood within 1 h after blood draw. Urine samples of three benign bone tumor patients were not obtained. All samples were stored at −80 °C until use in the assay.

Gas Chromatography−Time-of-Flight Mass Spectrometry (GC-TOFMS) Spectral Acquisition of Serum Samples and Data Pretreatment. Serum metabolites were subjected to trimethylsilyl derivatization and analyzed by GC-TOFMS according to the procedures outlined in our previously published paper with minor modifications.[16] Briefly, two internal standard solutions (10 μL of L-2-chlorophenylalanine in water, 0.3 mg/mL; 10 μL of heptadecanoic acid in methanol, 1 mg/mL) were spiked into a 100-μL aliquot of serum sample. A mixture of methanol/chloroform (3:1) (300 μL) was used to extract the metabolites from the serum. After a vortexing period of 30 s and storage for 10 min at −20 °C, the samples were centrifuged at 12 000*g* for 10 min. An aliquot of the 300-μL supernatant was vacuum-dried at room temperature in a glass vial. The residue was derivatized with 80 μL of methoxyamine (15 mg/mL in pyridine) at 30 °C for 90 min, and followed by 80 μL of BSTFA (1%TMCS) at 70 °C for 60 min.

Each 1-μL of derivatized solution was injected into an Agilent 6890N gas chromatograph coupled with a Pegasus HT time-of-flight mass spectrometer (Leco Corporation, St. Joseph, MI) at 270 °C in splitless mode. Metabolite separation was achieved on a DB-5 ms capillary column (30 m × 250 μm i.d., 0.25-μm film thickness; Agilent J&W Scientific, Folsom, CA) with helium as the carrier gas at a constant flow rate of 1.0 mL/min. The GC oven temperature programming was started at 80 °C and maintained for 2 min, followed by 10 °C/min ramps to 180 °C, 5 °C/min to 240 °C, and 25 °C/min to 290 °C, and a final 9 min maintenance at 290 °C. The temperature of transfer interface and ion source was set to 260 and 200 °C, respectively. Electron impact ionization (70 eV) was used. Mass data was collected after a 5 min solvent delay by Leco ChromaTOF software (v3.30, Leco Co., CA) at full scan mode (m/z 30−600) with an acquisition rate of 20 spectrum/second.

All GC/TOFMS files were converted to CDF format via ChromaTOF software. CDF files were processed with custom scripts (revised Matlab toolbox HDA, developed by Jonsson, et al.[17,18]) in MATLAB 7.0 (The MathWorks, Inc.) for data pretreatment procedures, such as baseline correction, denoising, smoothing and alignment, time-window splitting, and peak feature extraction (based on multivariate curve resolution algorithm).[18] Three-dimensional output data results were obtained with arbitrary peak index information (retention time−m/z pairs), sample names (observations), and peak intensity (variables).

GC-MS Spectral Acquisition of Urine Samples and Data Pretreatment. Urine samples were derivatized with ethyl chloroformate (ECF) and analyzed by GC-MS following our previously developed procedures with minor modifications.[19] A 600-μL aliquot of urine sample was used with 100 μL of L-2-chlorophenylalanine (0.1 mg/mL in water) as an internal standard. Then, the sample was added to 400 μL of anhydrous ethanol, 100 μL of pyridine, and 50 μL of ECF, and sonicated at 40 kHz for 60 s. After adding 300 μL of chloroform, the mixture was vortexed and the aqueous layer was adjusted to pH 9−10 using 100 μL of NaOH (7 M). The derivatization was repeated by adding another 50 μL of ECF. After vortexing for 30 s, the sample was centrifuged at 1900*g* for 10 min. The chloroform layer containing derivatives was dried with anhydrous sodium sulfate for subsequent GC-MS analysis.

Each 1-μL chloroform layer containing ECF-derivatives was injected into a HP-5MS capillary column (30 m × 250 μm i.d., 0.25-μm film thickness; Agilent J&W Scientific, Folsom, CA) and conducted on a hyphenated Agilent 6890N GC/5975B inert MSD (Agilent Technologies, Santa Clara, CA). The sample was injected at 260 °C in splitless mode. Helium was used as the carrier gas with a constant flow rate of 1.0 mL/min. The GC oven was started at 80 °C for 2 min, then the temperature was increased 10 °C/min to 140 °C, 4 °C/min to 180 °C, and 10 °C/min to 280 °C and maintained at 280 °C for 3 min. The transfer interface temperature was set to 260 °C. The mass setting was set in full scan (m/z 30−500) mode with electron impact ionization (70 eV). The ion source temperature was set at 200 °C. The data was collected after a 3 min solvent delay.

The data from the GC/MS analysis was converted into CDF format via the data analysis interface of the Agilent Instrument (Agilent Technologies). Then, the data was directly processed using our custom scripts in MATLAB 7.0 (The MathWorks, Inc.), to carry out baseline correction, peak deconvolution and alignment, exclusion of the internal standard peak and all known artifact peaks from column bleed and derivatization, and normalization to the total sum of the chromatogram.[20] A 3-dimensional resulting output data was obtained with arbitrary

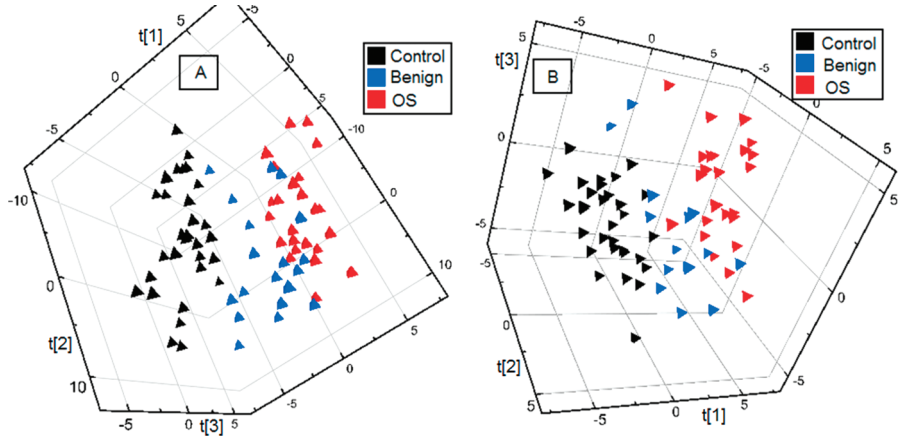

Figure 1. PLS scores plots generated from serum and urine sample data sets of all three groups. (A) PLS scores plot from serum metabonomic data set (3 components, $R2X_{(cum)} = 0.322$, $R2Y_{(cum)} = 0.826$, $Q2_{(cum)} = 0.525$); (B) PLS scores plot from urine metabonomic data set (3 components, $R2X_{(cum)} = 0.265$, $R2Y_{(cum)} = 0.865$, $Q2_{(cum)} = 0.489$).

peak index information (retention time−m/z pairs), sample names (observations), and peak intensity (variables).

Statistical Analysis. The resulting 3-dimensional data sets from GC-TOFMS and GC-MS analysis were introduced into SIMCA-P 11.5 software (Umetrics, Umeå, Sweden) for multivariate statistics, as previously reported.[21] Prior to multivariate statistics, the data was mean-centered and pareto-scaled. The unsupervised principal component analysis (PCA) was first used in all samples to see the general separation and find the outliers. Then, supervised partial least-squares (PLS) and orthogonal partial least-squares-discriminant analyses (OPLS-DA) were performed. To guard against model overfitting, the supervised models were validated with a 200 times permutation test.

Identification of Differential Metabolites. Serum and urine differential variables associated with OS and benign bone tumors were selected based on a threshold of variable importance in the projection (VIP) value (VIP > 1) from a typical 7-fold cross-validated OPLS-DA model. In parallel, these differential metabolites from the OPLS-DA model were validated at a univariate level using Student's t test. The critical p-value of the test was set to 0.05 in this study. The corresponding fold change shows how the metabolites varied from diseased individuals compared with those of the healthy controls. The barplots of some typical differential metabolites were conducted in PASW Statistics 18 software (Chicago, IL). Compound identification was performed in AMDIS software with NIST library 2005, with a similarity threshed of 70%. Finally, over 70% of them were verified by reference compounds.

Results

Metabonomic Analysis of Serum Samples. A total of 260 aligned individual peaks were obtained from serum samples after the removal of internal standards and known artificial peaks. The age difference in the study subjects may contribute to the intergroup separation and, therefore, become a cause of prejudice in the identification of differential metabolites in a metabonomic study. In our current study, most of the ages of participants range from 14 to 30. The mean age of the benign tumor group is actually influenced by several patients whose ages are greater than 60 years old, see Table 1. In the OS group, the ages of these participants were mainly from 14 to 30 with 3 patients older than 30 years old (Table 1). To check the age diversity and its contribution to the metabonomic profiles, we performed a PCA model of the serum metabonomic data of each group, and it appears that the profiles were not separated by their age difference (Supporting Information I Figure 1A and 1B) (SI Figure 6A). Therefore, the separation here should be mainly contributed by the biochemical variations associated with bone tumors morbidity.

PCA scores plot from all the samples using 5 components ($R2X_{(cum)} = 0.576$, $Q2_{(cum)} = 0.431$) showed a separation tendency between the control samples and OS individuals, while the benign samples were dispersed among the other two sample groups (Supporting Information Figure 2A). Similar results were obtained in the 3-D PLS model (3 components, $R2X_{(cum)} = 0.322$, $R2Y_{(cum)} = 0.826$, $Q2_{(cum)} = 0.525$) (Figure 1A), and validated by a permutation test illustrated in Supporting Information Figure 3A. PCA scores plot of each two-group comparison was shown in Supporting Information Figure 2B−D. We further used OPLS-DA models to compare between the control and OS samples, control and benign bone tumor samples, and OS and benign bone tumors with satisfactory modeling and predictive abilities (Figure 2A−C). All the OPLS-DA models were validated with a 200 times of permutation test, as all the $R2_{(cum)}$ and $Q2_{(cum)}$ values calculated from the permuted data were lower than the original ones in the validation plot and all the $Q2_{(cum)}$ intercepted the y-axis below zero (Supporting Information Figure 3B−D).

To test the prediction ability of this OPLS-DA model, 75% of samples from each group were used as the training set and the rest of the samples were used as the test set. From the t-predict scores plots (Supporting Information Figure 4A−C), all the samples in the test set were correctly distributed to the control group or OS group in the OPLS-DA model between control and OS group (using a cutoff value of 0), while 2 samples in the test set (1 from benign tumor group and 1 from OS or control group) were assigned to the wrong groups. Among the statistically significant variables identified using VIP values (VIP > 1) in the OPLS-DA model and the Student's t test ($p < 0.05$) (Table 2), 29 differential metabolites were annotated using NIST databases and 20 were confirmed using reference standards. A number of metabolites showed increased concentration in OS and benign tumor patients, such as cystine and 2-hydroxybutyrate, while several others, such

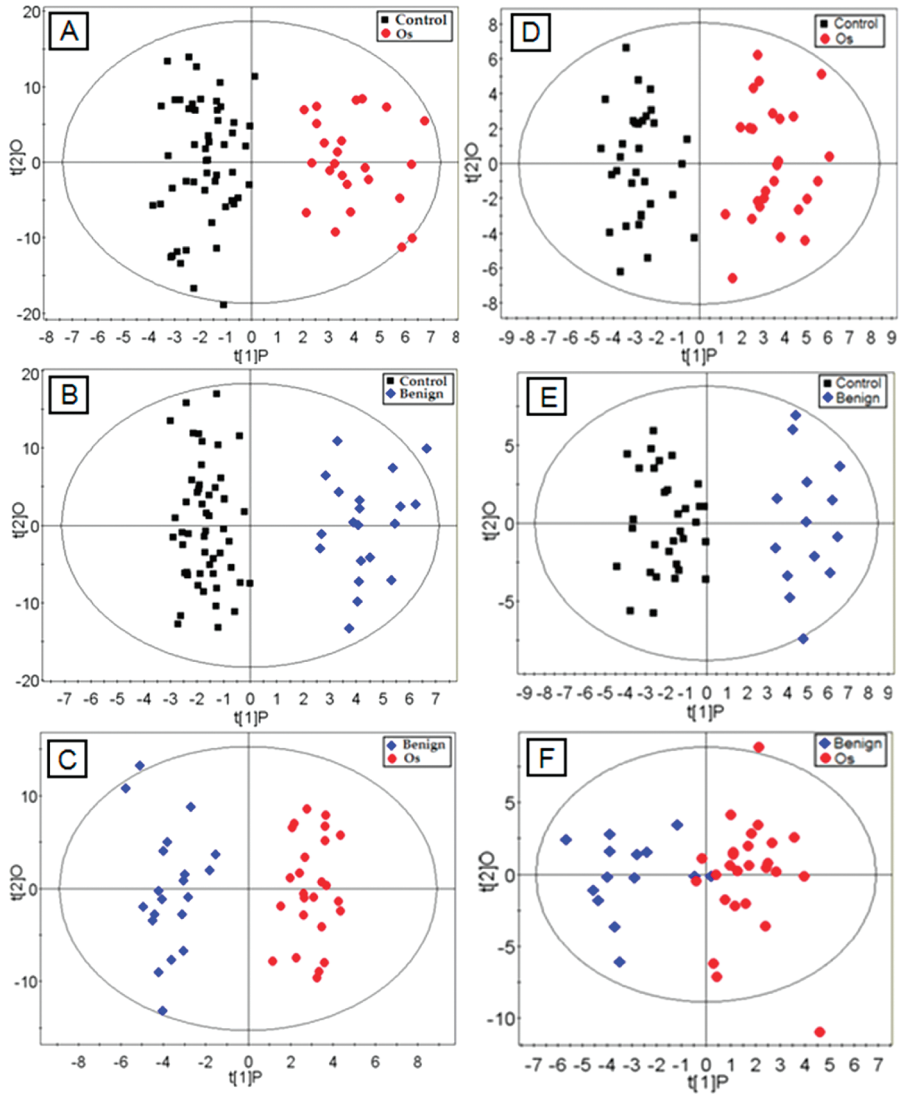

Figure 2. OPLS scores plots between each two groups. (A) OPLS-DA scores plot for control and OS group (serum, one predictive component and two orthogonal components, $R2X_{(cum)} = 0.335$, $R2Y_{(cum)} = 0.92$, $Q2_{(cum)} = 0.806$); (B) OPLS-DA scores plot for control and benign bone tumor group (serum, one predictive component and two orthogonal components, $R2X_{(cum)} = 0.461$, $R2Y_{(cum)} = 0.881$, $Q2_{(cum)} = 0.605$); (C) OPLS-DA scores plot for benign bone tumor and OS group (serum, one predictive component and three orthogonal components, $R2X_p = 0.163$, $R2X_{(cum)} = 0.47$, $R2Y_{(cum)} = 0.939$, $Q2_{(cum)} = 0.546$); (D) OPLS-DA scores plot for control and OS group (urine, one predictive component and two orthogonal components, $R2X_{(cum)} = 0.302$; $R2Y_{(cum)} = 0.882$; $Q2_{(cum)} = 0.6$); (E) OPLS-DA scores plot for control and benign bone tumor group (urine, one predictive component and two orthogonal components, $R2X_{(cum)} = 0.348$; $R2Y_{(cum)} = 0.881$; $Q2_{(cum)} = 0.509$); (F) PCA scores plot for benign bone tumor and OS group (urine, one predictive component and one orthogonal components, $R2X_{(cum)} = 0.192$; $R2Y_{(cum)} = 0.794$; $Q2_{(cum)} = 0.292$).

as malate and dodecanoic acid, were observed in decreased levels in the two patient groups, as depicted in Figure 3A−D.

Metabonomic Analysis of Urine Samples. A total of 180 individual peaks were detected from the urine spectra. Similar to serum metabonomic analysis, we first used PCA model to evaluate the impact of age difference on the metabonomic profiles of benign bone tumor group and OS group, respectively. No valid PCA model was obtained between higher and lower ages for benign bone tumor group and the OS group, respectively, in the urine data set. After removal of the two outliers from the benign bone tumor group, a PCA model was able to demonstrate the separation tendency between OS patients and control samples in the scores plot, while the benign tumors clustered together with the OS (5 components, $R2X_{(cum)} = 0.46$, $R2Y_{(cum)} = 0.196$) (Supporting Information Figure 5A). Clear intergroup separations were obtained from a three components PLS model ($R2X_{(cum)} = 0.265$, $R2Y_{(cum)} = 0.865$, $Q2_{(cum)} = 0.489$) among the three groups with few overlaps (Figure 1B). The permutation test was provided in Supporting Information Figure 6A. The OPLS-DA models were performed which showed distinct separation between each pair of groups, control and OS (one predictive component and two orthogonal components, $R2X_{(cum)} = 0.302$; $R2Y_{(cum)} = 0.882$; $Q2_{(cum)} = 0.6$, Figure 2D), control and benign tumors (one predictive component and two orthogonal components, $R2X_{(cum)} = 0.348$; $R2Y_{(cum)} = 0.881$; $Q2_{(cum)} = 0.509$, Figure 2E), and OS and benign tumors (one predictive component and one orthogonal components, $R2X_{(cum)} = 0.192$; $R2Y_{(cum)} = 0.794$; $Q2_{(cum)} = 0.292$, Figure 2F). Permutation tests supported the validity of these three OPLS-DA models (Supporting Information Figure 6B−D).

Table 2. Serum Differential Metabolites Obtained from Control, OS and Benign Bone Tumor Samples

		OS vs control			benign vs control			OS vs benign			
no.	compound name	VIP[a]	p^b	FC[c]	VIP[a]	p^b	FC[c]	VIP[a]	p^b	FC[c]	related metabolism
1	Cystine[d]	3.16	2.32×10^{-7}	2.09	3.84	1.87×10^{-7}	2.25				Glutathione metabolism
2	2-hydroxybutyrate[d]	2.28	1.84×10^{-3}	2.09	3.05	6.56×10^{-4}	1.95				Glutathione metabolism
3	γ-aminobutyrate[d]	1.81	4.72×10^{-3}	−1.57				1.43	4.63×10^{-2}	−1.34	Glutamate metabolism
4	Glutamate[d]				2.81	6.19×10^{-4}	2.04	1.3	9.20×10^{-2}	−1.59	Glutamate metabolism
5	Malate[d]	3.42	4.80×10^{-10}	−2.46	2.47	3.51×10^{-4}	−1.57	1.67	2.97×10^{-2}	−1.57	TCA cycle
6	Fumarate[d]	2.02	4.02×10^{-4}	−1.58	2.66	9.20×10^{-5}	−1.81				TCA cycle
7	α-ketoglutarate[d]							1.64	4.70×10^{-2}	−1.48	TCA cycle
8	Pyruvate[d]	2.17	1.49×10^{-4}	−1.63							Glycolysis
9	Lactate[d]	1.59	8.22×10^{-3}	−1.30				1.81	1.34×10^{-2}	−1.39	Glycolysis
10	Dodecanoate[d]	1.64	9.36×10^{-3}	−2.76	1.84	2.53×10^{-2}	−2.58				Fatty acid metabolism
11	Arachidonate[d]	1.40	2.51×10^{-2}	−1.28				1.45	2.99×10^{-2}	−1.26	Fatty acid metabolism
12	Glycerate[d]	1.11	3.68×10^{-2}	−1.38							Glycerolipid metabolism
13	Glycerol, phosphate	2.73	7.47×10^{-6}	−1.53				1.38	6.07×10^{-2}	−1.3	Glycerolipid metabolism
14	Sucrose[d]	3.04	7.12×10^{-8}	−23.3	3.25	1.55×10^{-6}	−29.7				Sucrose metabolism
15	Fructose[d]							1.64	4.86×10^{-2}	−1.58	Sucrose metabolism
16	Asparagine[d]	1.49	5.35×10^{-2}	−1.43				1.67	1.99×10^{-2}	−1.63	Aspartate metabolism
17	Beta-alanine[d]				1.30	3.30×10^{-2}	1.53	2.26	9.62×10^{-4}	−1.91	Aspartate metabolism
18	Ribitol	1.53	3.36×10^{-2}	1.50	3.04	1.42×10^{-4}	2.10				Ribose metabolism
19	Ribose				1.79	1.98×10^{-2}	1.43	2.28	3.77×10^{-3}	−1.59	Pentose phosphate pathway
20	Inosine	2.57	3.84×10^{-5}	5.19	2.52	8.00×10^{-4}	11.22				Purine metabolism
21	Ornithine[d]							1.35	3.34×10^{-2}	−1.38	Urea cycle
22	Creatinine[d]	1.71	2.76×10^{-2}	1.22	2.25	1.46×10^{-2}	1.30				Others
23	Erythrose	1.29	3.60×10^{-2}	−1.51				1.98	1.24×10^{-2}	−1.63	Others
24	Glucopyranose	1.49	3.78×10^{-2}	1.79				1.68	1.13×10^{-2}	2.63	Others
25	Galactopyranose	1.53	3.79×10^{-2}	1.77				1.75	8.67×10^{-3}	2.73	Others
26	2-Piperidine Carboxylate[d]				2.09	3.55×10^{-3}	2.04	1.64	1.68×10^{-2}	−1.96	Others
27	N-Acetylglutamine							1.61	4.35×10^{-2}	1.64	Others
28	2-oxo-3-methyl- pentanate[d]				1.19	5.85×10^{-2}	−1.20	1.46	2.76×10^{-2}	1.29	Others
29	2-Ketoisocapronate				1.58	3.31×10^{-2}	−1.28				Others

[a] Variable importance in the projection (VIP) was obtained from OPLS-DA with a threshold of 1.0. [b] The *p*-value was calculated from Student *t* test. [c] Fold change was calculated from the arithmetic mean values of each group. Fold change with a positive value indicates a relatively higher concentration present in OS or benign tumor samples while a negative value means a relatively lower concentration as compared to the healthy controls or benign tumor samples (between OS and benign bone tumor). [d] Metabolites verified by reference compounds, other were directly obtained from library searching.

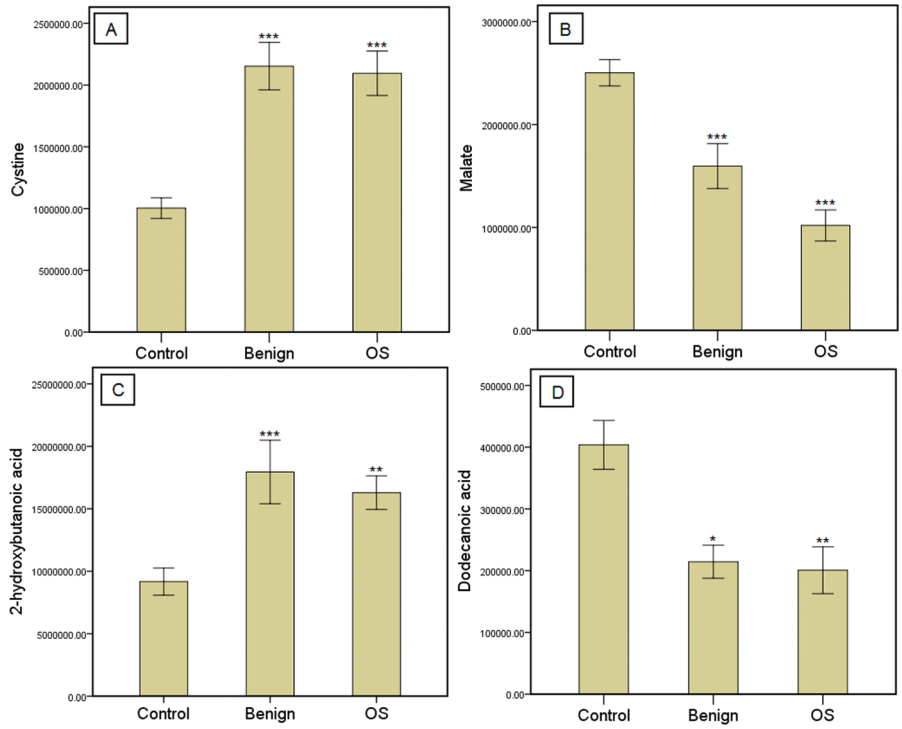

Figure 3. Barplots of typical differential metabolites obtained from serum samples. (A) cystine; (B) malate; (C) 2-hydroxybutanoic acid; (D) dodecanoic acid. (*$p < 0.05$, **$p < 0.01$, ***$p < 0.001$; *p*-values were calculated by comparing OS or benign bone tumor samples with control ones.)

The prediction models were also performed between each two groups using OPLS-DA model by taking about 75% of the samples as training set and the rest of samples as test set. As shown in Supporting Information Figure 7A−C, the prediction model between control and OS patients can correctly predict all the samples in the test set. However, 2 samples from OS test group were predicted as benign tumor in the prediction model between OS and benign bone tumor patients, and 1

Table 3. Urine Differential Metabolites Obtained from Control, OS and Benign Bone Tumor Samples

		OS vs control			benign vs control			OS vs benign			
no.	compound name	VIP[a]	p^b	FC[c]	VIP[a]	p^b	FC[c]	VIP[a]	p^b	FC[c]	related metabolism
1	Cystine[d]	1.97	1.38×10^{-5}	3.01				1.82	1.88×10^{-2}	2.14	Glutathione metabolism
2	Cysteine[d]				1.31	1.60×10^{-2}	1.46				Glutathione metabolism
3	Isocitrate[d]	1.02	4.37×10^{-2}	−1.59							TCA cycle
4	Putrescine	2.07	7.14×10^{-6}	2.86				2.06	7.19×10^{-3}	2.42	Polyamine metabolism
5	Hippurate[d]	1.38	2.22×10^{-3}	−2.11	1.94	1.81×10^{-4}	−5.36	1.40	7.39×10^{-2}	2.54	Gut flora metabolism
6	p-hydroxyphenyl Propionate				2.04	6.97×10^{-5}	2.99				Gut flora metabolism
7	Aspartate[d]	1.88	2.46×10^{-5}	1.62	1.75	8.90×10^{-4}	1.53				Arginine and proline metabolism
8	Proline[d]	1.60	3.19×10^{-4}	1.60	1.48	5.74×10^{-3}	3.10	2.49	6.93×10^{-2}	−1.93	Arginine and proline metabolism
9	Valine[d]	1.65	2.76×10^{-4}	1.40	1.90	2.62×10^{-4}	1.44				Valine, leucine and isoleucine degradation
10	Leucine[d]	1.47	8.38×10^{-4}	1.39	1.20	2.84×10^{-2}	1.35				Valine, leucine and isoleucine degradation
11	Isoleucine[d]	1.23	8.42×10^{-3}	1.25	1.34	1.31×10^{-2}	1.32				Valine, leucine and isoleucine degradation
12	Phenylalanine[d]	1.60	3.00×10^{-4}	1.51	1.26	2.08×10^{-2}	1.41				Phenylalanine and tyrosine metabolism
13	Tyrosine[d]	1.34	2.52×10^{-3}	1.42							Phenylalanine and tyrosine metabolism
14	Homovanilate[d]				1.55	3.77×10^{-3}	2.56	2.23	3.27×10^{-3}	−2.83	Tyrosine Metabolism
15	Tryptophane[d]	1.25	7.07×10^{-3}	1.70	1.23	2.42×10^{-2}	1.36				Tryptophan metabolism
16	Alanine[d]				1.42	8.39×10^{-3}	1.76				Alanine metabolism
17	Glycine[d]				1.29	1.76×10^{-2}	1.70	2.34	1.93×10^{-3}	−1.82	Glycine, serine and threonine metabolism
18	Histidine[d]				1.18	3.06×10^{-2}	2.37				Histidine Metabolism
19	Hexadecanoate[d]				1.33	1.38×10^{-2}	1.58				Fatty acid Metabolism
20	Acetylcitrate	1.72	3.83×10^{-4}	1.49	1.52	4.58×10^{-3}	1.40				Others
21	Poline-valine	2.18	1.62×10^{-6}	2.38				2.28	2.55×10^{-3}	2.08	Others

[a] Variable importance in the projection (VIP) was obtained from OPLS-DA with a threshold of 1.0. [b] The *p*-value was calculated from Student *t* test. [c] Fold change was calculated from the arithmetic mean values of each group. Fold change with a positive value indicates a relatively higher concentration present in OS or benign tumor samples while a negative value means a relatively lower concentration as compared to the healthy controls or benign tumor samples (between OS and benign bone tumor). [d] Metabolites verified by reference compounds, other were directly obtained from library searching.

sample from control test group was predicted as benign tumor in the prediction model between control and benign bone tumor patients.

Twenty-one identified variables were selected according to the VIP values (VIP > 1) from the OPLS-DA models and *p*-values from Student's *t* test ($p < 0.05$). These urinary metabolites were annotated by the NIST library and 17 were confirmed by reference compounds (Table 3). Similar to the serum results, cystine was found significantly increased in the urine samples of the OS and benign bone subjects. Higher levels of other amino acids, such as valine and phenylalanine, were also observed in the OS and benign tumors, while lower levels of hippurate were detected in the OS and benign tumor samples. The barplots of cystine, putresine, hippurate, and phenylalanine were demonstrated in Figure 4.

Discussion

The GC-MS based metabolomics approach can capture the differentially expressed metabolites associated with OS morbidity. In this study, we identified 29 differential metabolites in the serum samples and 21 differential metabolites in the urine samples. Our results showed the potential of using metabolomics to discriminate the OS from healthy individuals and benign bone tumors.

Significantly increased level of cystine was observed both in the serum and urine samples from OS and benign bone tumor patients as compared to the healthy controls. A higher serum level of glutamate was detected in benign tumor patients, but not in the OS patients. The elevated cystine in serum may increase the activity of cystine/glutamate antiporter, which mediates the incorporation of extracellular cystine into the cytoplasmic location for the biosynthesis of glutathione in exchange for intracellular glutamate.[22] The activated antiporter would result in an increased intracellular cystine level, which would then increase the glutathione biosynthesis level. However, the higher level of glutamate in benign bone tumor patients may offset the cystine induced cystine/glutamate antiporter increase to some extent. The serum 2-hydroxybutanoic acid, a byproduct of the methionine to glutathione pathway,[23] was found differentially expressed, at the highest level in OS patients and the lowest level detected in the control samples. Since glutamate was reported to suppress osteoclastogenesis through the retrograde operation of the antiporter to lead to the reduction of intracellular glutathione,[24] the significantly higher levels of cystine and 2-hydroxybutanoic acid may be associated with increased osteoclastogenesis in OS patients. In addition, a significantly lower level of γ-aminobutyric acid (GABA) in serum was observed in the OS patients relative to the healthy controls. As the metabolic product of glutamate, the decreased concentration of GABA may be a further indication of disturbed glutamate metabolism in OS patients.

Decreased serum concentrations of fumarate and malate were observed both in OS patients and in benign bone tumor patients. Fumarate and malate are intermediates in the TCA cycle and catalyzed by succinate dehydrogenase (SDH) and fumarate hydratase (FH), both located in mitochondria. The depletion of these two metabolites may suggest a lowered activity of SDH and FH in the patients, which is supported by a report that views the disordered activity of SDH and FH as the link between mitochondrial dysfunction and cancer.[25] The decreased level of isocitrate in the OS urine may further support the speculation of an impaired TCA cycle in the OS patients.

Both pyruvate and lactate, the intermediates and end-products of glycolysis, were found significantly decreased in the OS serum samples. This is not consistent with metabolic changes in other cancers. As the Warburg effect describes, cancer cells result in an increase of glycolysis,[26] which leads to down-regulated TCA cycle and increased lactate level. Such a unique alteration may constitute a characteristic metabolite

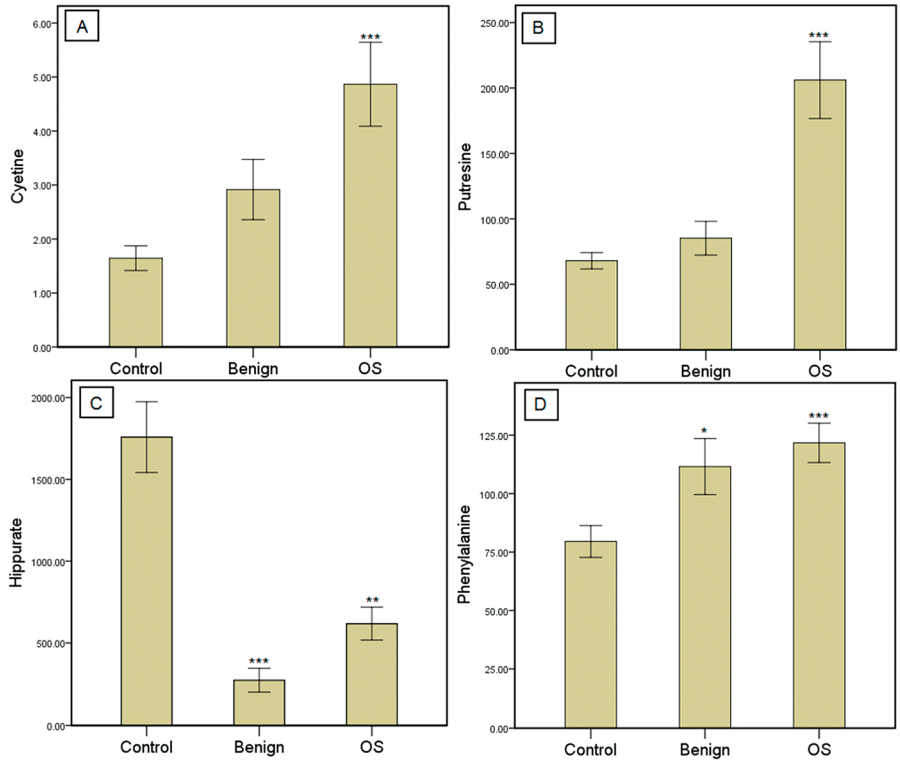

Figure 4. Barplots of typical differential metabolites obtained from urine samples. (A) cystine; (B) putresine; (C) hippurate; (D) phenylalanine. (*$p < 0.05$, **$p < 0.01$, ***$p < 0.001$; p-values were calculated by comparing OS or benign bone tumor samples with control ones.)

signature that will differentiate OS from benign tumors and other cancers.

Several metabolites in lipid metabolism, such as arachidonic acid, dodecanoic acid, and glycerate, were observed significantly decreased in the serum of OS patients, suggesting an altered lipid metabolism associated with OS morbidity. Furthermore, as the precursor to prostaglandins, arachidonic acid plays an important role in regulating bone metabolism.[27] Previous reports have shown that the tumor necrosis factor alpha (TNF-alpha) in human osteoblastic osteosarcoma cell line can stimulate cyclooxygenase and lipoxygenase pathways of arachidonic acid metabolism in a dose-dependent manner in cells.[28] Therefore, the down-regulated lipid metabolites may be associated with altered bone metabolism in OS patients.

A significantly lower level of hippurate was observed in the urine of both OS and benign tumor patients. Hippurate is synthesized from benzoic acid and glycine in mitochondrial and catalyzed by benzoyl-CoA synthetase and benzoyl-CoA/glycine *N*-acyltransferase.[29,30] Since benzoic acid is mainly generated via gut microflora, the variation of hippurate is usually believed to be associated with gut flora metabolism.[31] However, in this study, the alternation of benzoic acid was not observed, and the decreased level of hippurate in the urine is therefore presumably due to the impaired mitochondrial enzymes. This may further support the speculation of a disordered mitochondrial metabolism associated OS morbidity.

The levels of several sugars or polyol, such as sucrose, ribose, and ribitol fluctuated significantly in the serum of OS patients and benign bone tumor patients. Ribitol was reported to be a metabolic end-product of ribose in human fibroblasts and erythrocytes catalyzed by pentitol dehydrogenase.[32] The increased level of ribitol in bone tumor patients (benign and OS) may suggest an increased activity of pentitol dehydrogenase associated with OS morbidity, although the altered sugar and polyol profiles are yet to be elucidated.

Putrescine, one of the polyamines, was also detected in higher concentration in the urine of OS patients. Reports have shown that polyamines may modulate the RNA expression of the cancer-related gene cyclooxygenase-2 (COX-2) through the polyamine-dependent gene, eIF 5A.[33] Reports also indicated that repressed intercellular polyamine levels by polyamine synthesis inhibitor could inhibit cell growth and induce apoptotic cell death in human osteosarcoma cell lines.[34] Additionally, several amino acids, such as phenylalanine, valine, and proline were also observed significantly higher in the urine samples from OS patients and benign tumor patients, suggesting an increased amino acid metabolism along with the down-regulated glycolysis and lipid metabolism in the OS and benign bone tumor patients to compensate energy supply. For example, all the three branched-chain amino acids, valine, leucine, and isoleucine, were observed in higher levels in the bone tumor patients, as these metabolites can be converted either into acetyl-CoA or succinyl-CoA to enter the citric acid cycle for energy generation.

In summary, the noninvasive, metabonomic approach is able to acquire characteristic metabolic profiles in serum and urine of osteosarcoma patients. Differential metabolites identified from metabonomic analysis suggest a disrupted energy metabolism in OS patients, as characterized by significantly down-regulated TCA cycle and glycolysis, down-regulated lipid metabolism, dysregulated sugar levels, and upregulated amino acid metabolism. Additionally, an increased activity of glutathione metabolism, and increased polyamine metabolism also contributed to a characteristic metabolic profile of OS patients.

Acknowledgment. This work was funded by the National Basic Research Program of China (Project number 2007CB914700).

Supporting Information Available: PCA scores plots generated from serum samples with showing the age of each patient; PCA scores plots of the metabolite profiles of serum samples; permutation test for the supervised models of serum metabolomic study; t-prediction scores plot of serum samples; PCA scores plots of the metabolite profiles of serum samples; permutation test for the supervised models of urine metabolomic study, t-prediction scores plot of urine samples. This material is available free of charge via the Internet at http://pubs.acs.org.

References

(1) Folio, C.; Mora, M. I.; Zalacain, M.; Corrales, F. J.; Segura, V.; Sierrasesumaga, L.; Toledo, G.; San-Julian, M.; Patino-Garcia, A. Proteomic analysis of chemonaive pediatric osteosarcomas and corresponding normal bone reveals multiple altered molecular targets. *J. Proteome Res.* **2009**, *8* (8), 3882–3888.

(2) Picci, P. Osteosarcoma (Osteogenic sarcoma). *Orphanet. J. Rare Dis.* **2007**, *2*, 4.

(3) Sandberg, A. A.; Bridge, J. A. Updates on the cytogenetics and molecular genetics of bone and soft tissue tumors: osteosarcoma and related tumors. *Cancer Genet. Cytogenet.* **2003**, *145* (1), 1–30.

(4) Sluga, M.; Windhager, R.; Lang, S.; Heinzl, H.; Bielack, S.; Kotz, R. Local and systemic control after ablative and limb sparing surgery in patients with osteosarcoma. *Clin. Orthop. Relat. Res.* **1999**, (358), 120–127.

(5) Toguchida, J.; Ishizaki, K.; Sasaki, M. S.; Nakamura, Y.; Ikenaga, M.; Kato, M.; Sugimot, M.; Kotoura, Y.; Yamamuro, T. Preferential mutation of paternally derived RB gene as the initial event in sporadic osteosarcoma. *Nature* **1989**, *338* (6211), 156–158.

(6) Lopez-Guerrero, J. A.; Lopez-Gines, C.; Pellin, A.; Carda, C.; Llombart-Bosch, A. Deregulation of the G1 to S-phase cell cycle checkpoint is involved in the pathogenesis of human osteosarcoma. *Diagn. Mol. Pathol.* **2004**, *13* (2), 81–91.

(7) Abbott, D. W.; Holt, J. T. Finkel-Biskis-Reilly mouse osteosarcoma virus v-fos inhibits the cellular response to ionizing radiation in a myristoylation-dependent manner. *J. Biol. Chem.* **1997**, *272* (22), 14005–14008.

(8) Ochi, K.; Daigo, Y.; Katagiri, T.; Nagayama, S.; Tsunoda, T.; Myoui, A.; Naka, N.; Araki, N.; Kudawara, I.; Ieguchi, M.; Toyama, Y.; Toguchida, J.; Yoshikawa, H.; Nakamura, Y. Prediction of response to neoadjuvant chemotherapy for osteosarcoma by gene-expression profiles. *Int. J. Oncol.* **2004**, *24* (3), 647–55.

(9) Qiu, Y.; Cai, G.; Su, M.; Chen, T.; Zheng, X.; Xu, Y.; Ni, Y.; Zhao, A.; Xu, L. X.; Cai, S.; Jia, W. Serum metabolite profiling of human colorectal cancer using GC-TOFMS and UPLC-QTOFMS. *J. Proteome Res.* **2009**, *8* (10), 4844–4850.

(10) Qiu, Y.; Cai, G.; Su, M.; Chen, T.; Liu, Y.; Xu, Y.; Ni, Y.; Zhao, A.; Cai, S.; Xu, L. X.; Jia, W. Urinary metabonomic study on colorectal cancer. *J. Proteome Res.* , *9* (3), 1627–1634.

(11) Sreekumar, A.; Poisson, L. M.; Rajendiran, T. M.; Khan, A. P.; Cao, Q.; Yu, J.; Laxman, B.; Mehra, R.; Lonigro, R. J.; Li, Y.; Nyati, M. K.; Ahsan, A.; Kalyana-Sundaram, S.; Han, B.; Cao, X.; Byun, J.; Omenn, G. S.; Ghosh, D.; Pennathur, S.; Alexander, D. C.; Berger, A.; Shuster, J. R.; Wei, J. T.; Varambally, S.; Beecher, C.; Chinnaiyan, A. M. Metabolomic profiles delineate potential role for sarcosine in prostate cancer progression. *Nature* **2009**, *457* (7231), 910–914.

(12) Rocha, C. M.; Barros, A. S.; Gil, A. M.; Goodfellow, B. J.; Humpfer, E.; Spraul, M.; Carreira, I. M.; Melo, J. B.; Bernardo, J.; Gomes, A.; Sousa, V.; Carvalho, L.; Duarte, I. F. Metabolic profiling of human lung cancer tissue by H-1 high resolution magic angle spinning (HRMAS) NMR spectroscopy. *J. Proteome Res.* , *9* (1), 319–332.

(13) Kim, K.; Aronov, P.; Zakharkin, S. O.; Anderson, D.; Perroud, B.; Thompson, I. M.; Weiss, R. H. Urine metabolomics analysis for kidney cancer detection and biomarker discovery. *Mol. Cell. Proteomics* **2009**, *8* (3), 558–570.

(14) Marchesi, J. R.; Holmes, E.; Khan, F.; Kochhar, S.; Scanlan, P.; Shanahan, F.; Wilson, I. D.; Wang, Y. Rapid and noninvasive metabonomic characterization of inflammatory bowel disease. *J. Proteome Res.* **2007**, *6* (2), 546–551.

(15) van Doorn, M.; Vogels, J.; Tas, A.; van Hoogdalem, E. J.; Burggraaf, J.; Cohen, A.; van der Greef, J. Evaluation of metabolite profiles as biomarkers for the pharmacological effects of thiazolidinediones in Type 2 diabetes mellitus patients and healthy volunteers. *Br. J. Clin. Pharmacol.* **2007**, *63* (5), 562–574.

(16) Li, H.; Xie, Z.; Lin, J.; Song, H.; Wang, Q.; Wang, K.; Su, M.; Qiu, Y.; Zhao, T.; Song, K.; Wang, X.; Zhou, M.; Liu, P.; Zhao, G.; Zhang, Q.; Jia, W. Transcriptomic and metabonomic profiling of obesity-prone and obesity-resistant rats under high fat diet. *J. Proteome Res.* **2008**, *7* (11), 4775–4783.

(17) Jonsson, P.; Gullberg, J.; Nordstrom, A.; Kusano, M.; Kowalczyk, M.; Sjostrom, M.; Moritz, T. A strategy for identifying differences in large series of metabolomic samples analyzed by GC/MS. *Anal. Chem.* **2004**, *76* (6), 1738–1745.

(18) Jonsson, P.; Johansson, A. I.; Gullberg, J.; Trygg, J.; A, J.; Grung, B.; Marklund, S.; Sjostrom, M.; Antti, H.; Moritz, T. High-throughput data analysis for detecting and identifying differences between samples in GC/MS-based metabolomic analyses. *Anal. Chem.* **2005**, *77* (17), 5635–5642.

(19) Qiu, Y.; Su, M.; Liu, Y.; Chen, M.; Gu, J.; Zhang, J.; Jia, W. Application of ethyl chloroformate derivatization for gas chromatography-mass spectrometry based metabonomic profiling. *Anal. Chim. Acta* **2007**, *583* (2), 277–283.

(20) Chen, M.; Su, M.; Zhao, L.; Jiang, J.; Liu, P.; Cheng, J.; Lai, Y.; Liu, Y.; Jia, W. Metabonomic study of aristolochic acid-induced nephrotoxicity in rats. *J. Proteome Res.* **2006**, *5* (4), 995–1002.

(21) Li, H.; Ni, Y.; Su, M.; Qiu, Y.; Zhou, M.; Qiu, M.; Zhao, A.; Zhao, L.; Jia, W. Pharmacometabonomic phenotyping reveals different responses to xenobiotic intervention in rats. *J. Proteome Res.* **2007**, *6* (4), 1364–1370.

(22) Lo, M.; Wang, Y. Z.; Gout, P. W. The x(c)- cystine/glutamate antiporter: a potential target for therapy of cancer and other diseases. *J. Cell Physiol.* **2008**, *215* (3), 593–602.

(23) Lord, R. S.; Bralley, J. A. Clinical applications of urinary organic acids. Part I: Detoxification markers. *Altern. Med. Rev.* **2008**, *13* (3), 205–215.

(24) Takarada, T.; Yoneda, Y. Pharmacological topics of bone metabolism: glutamate as a signal mediator in bone. *J. Pharmacol. Sci.* **2008**, *106* (4), 536–541.

(25) King, A.; Selak, M. A.; Gottlieb, E. Succinate dehydrogenase and fumarate hydratase: linking mitochondrial dysfunction and cancer. *Oncogene* **2006**, *25* (34), 4675–4682.

(26) Gatenby, R. A.; Gillies, R. J. Why do cancers have high aerobic glycolysis. *Nat. Rev. Cancer* **2004**, *4* (11), 891–899.

(27) Poulsen, R. C.; Moughan, P. J.; Kruger, M. C. Long-chain polyunsaturated fatty acids and the regulation of bone metabolism. *Exp. Biol. Med. (Maywood, NJ, U.S.)* **2007**, *232* (10), 1275–1288.

(28) Zhang, W. Y.; Dziak, R. Tumor necrosis factor alpha stimulates arachidonic acid metabolism in human osteoblastic osteosarcomal cells. *Prostaglandins, Leukotrienes Essent. Fatty Acids* **1996**, *54* (6), 427–431.

(29) Gatley, S. J.; Sherratt, H. S. A. Synthesis of hippurate from benzoate and glycine by rat-liver mitochondrial-submitchondrial locaization and kinetics. *Biochem. J.* **1977**, *166* (1), 39–47.

(30) Tremblay, G. C.; Qureshi, I. A. The Biochemistry and toxicology of benzoic acid metabolism and its relationship to the elimination of waste nitrogen. *Pharmacol. Ther.* **1993**, *60* (1), 63–90.

(31) Phipps, A. N.; Stewart, J.; Wright, B.; Wilson, I. D. Effect of diet on the urinary excretion of hippuric acid and other dietary-derived aromatics in rat. A complex interaction between diet, gut microflora and substrate specificity. *Xenobiotica* **1998**, *28* (5), 527–537.

(32) Huck, J. H. J.; Roos, B.; Jakobs, C.; van der Knaap, M. S.; Verhoeven, N. M. Evaluation of pentitol metabolism in mammalian tissues provides new insight into disorders of human sugar metabolism. *Mol. Genet. Metab.* **2004**, *82* (3), 231–237.

(33) Parker, M. T.; Gerner, E. W. Polyamine-mediated post-transcriptional regulation of COX-2. *Biochimie* **2002**, *84* (8), 815–819.

(34) Mori, K.; Hibasami, H.; Satoh, N.; Sonoda, J.; Yamasaki, T.; Tajima, M.; Higuchi, S.; Wakabayashi, H.; Kaneko, H.; Uchida, A.; Nakashima, K. Induction of apoptotic cell death in three human osteosarcoma cell lines by a polyamine synthesis inhibitor, methylglyoxal bis(cyclopentylamidinohydrazone) (MGBCP). *Anticancer Res.* **1997**, *17* (4A), 2385–2389.

PR100480R